Effect of ZnO surface defects on efficiency and stability of ZnO-based perovskite solar cells

Fangzhou Liu
Man Kwong Wong
Ho Won Tam
Aleksandra B. Djurišić
Alan M. C. Ng
Wai Kin Chan

Effect of ZnO surface defects on efficiency and stability of ZnO-based perovskite solar cells

Fangzhou Liu[a], Man Kwong Wong[a], Ho Won Tam[a], Aleksandra B. Djurišić*[a], Alan. M. C. Ng[b], Wai Kin Chan[c]

[a]Department of Physics, The University of Hong Kong, Hong Kong, China;
[b]Department of Physics, South University of Science and Technology of China, Shenzhen, China;
[c]Department of Chemistry, The University of Hong Kong, Hong Kong, China

ABSTRACT

ZnO as an alternative electron transport layer (ETL) material for perovskite solar cell applications has drawn increasing research interest due to its comparable energy levels to TiO_2, relatively high electron mobility, as well as its feasibility to be processed at low temperatures for potential applications in flexible devices. Nevertheless, ZnO based perovskite devices usually exhibit inferior performance and severe stability drawbacks which are related to the surface defects of ZnO ETL. In this study, to investigate the correlation between ZnO defect composition and resulting device performance, different approaches of preparing ZnO ETL are compared in terms of the perovskite morphology and device performance. In addition, direct manipulations of ZnO surface defects are performed by various surface treatments, and the photovoltaic performance of devices with ZnO ETL subjected to different surface treatments is compared. Surface modification of ZnO ETL by ethanolamine (EA) is demonstrated to efficiently enhance the photovoltaic performance of resulting ZnO based devices.

Keywords: perovskite, zinc oxide, solar cells, surface treatment

1. INTRODUCTION

Organometallic halide perovskite solar cells (PSCs) have demonstrated great potential as the next generation photovoltaic devices since the first reports in 2012.[1-3] Among various device architectures reported in the literature, TiO_2 is the most popular and viable choice for inorganic electron transporting layer (ETL) which has been extensively studied, with the highest energy converting efficiency of TiO_2 based devices exceeded 22% by 2016.[4] Despite the remarkable progress achieved in devices with TiO_2 as the electron transporting material, a growing research effort has been devoted on investigating alternative inorganic ETL materials, and among these candidates ZnO has drawn much attention in the recent years.[5-13] The research interest on ZnO as the alternative ETL candidate mainly roots from the fact that ZnO has similar energy levels and relatively higher electron mobility compared to TiO_2.[5-7] Moreover, its feasibility to be readily processed at low temperatures is favorable for fabrications of flexible devices.[7] Nevertheless, compared to TiO_2 based perovskite devices, inferior photovoltaic performance as well as severe stability drawbacks is generally observed in ZnO based perovskite devices.[8-10] In particular, perovskite films deposited on ZnO ETL are readily decomposed at 100 °C, which is not observed for perovskite films deposited on TiO_2.[9, 10] Such severe thermal instability of ZnO based devices is attributed to the proton transfer at ZnO/perovskite interface which is further related to the surface defects of ZnO.[10] It has also been reported that different preparation methods of ZnO ETL would affect the resulting device performance since the surface properties of ZnO are largely influenced by the synthesis processes.[11]

Regarding the issues mentioned above, attempts have been made to improve the stability of ZnO based devices by inserting an interlayer such as Al_2O_3[12] or Al-doped ZnO (AZO)[13] in between ZnO and perovskite layers to inhibit degradation of perovskites. However, the effect of directly modifying the surface of ZnO is seldom reported. Surface treatment is regarded as an efficient approach for directly manipulating the surface properties of various ZnO bulk- and nano-structures by passivating particular defect species at the surface of ZnO samples.[14] In addition, it has also been reported that an ethanolamine (EA) solution based surface treatment can efficiently reduce the energy barrier between

---

the ETL and the perovskite layer, as well as passivate the defects in the metal oxide for TiO_2 based PSCs.[15] Hence, in this study we will focus on both the influence of deposition methods of the ZnO ETL on the synthesis of perovskite layers and the resulting device performances, as well as the effect of surface treatment for ZnO based devices. ZnO compact layers were prepared by both solution process and electron beam deposition, and subjected to surface treatments with polyethyleneimine (PEI), polyvinylpyridine (PVP), and EA as the surfactants. Planar structured perovskite solar cells were fabricated based on ZnO ETL with different defect contents, and the influence on the device performance were investigated in detail.

2. EXPERIMENTAL DETAIL

2.1 Materials

Lead iodide (PbI_2, 99.9985%), N,N-Dimethylformamide (DMF, anhydrous, 99.9+%), and 2-propanol (anhydrous, 99.5+%) were obtained from Alfa Aesar. Zinc acetate (99.99%), 2-methoxyethanol (≥99.3%), ethanolamine (≥99.0%), polyethyleneimine (PEI), polyvinylpyrrolidone (PVP), bis (trifluoromethane) sulfonamide lithium salt (Li-TFSI, 99.95%), 4-tert butylpyridine (96%), chlorobenzene (≥99.5%), and acetonitrile (anhydrous, 99.8%) were purchased from Sigma Aldrich. Methylammonium iodide (MAI) was purchased from Dyesol. 2,2',7,7'-Tetrakis[N,N-di(4-methoxyphenyl)amino]-9,9'-spirobifluorene (spiro-OMeTAD) was purchased from Shenzhen Feiming Co., Ltd.

2.2 Preparation of ZnO ETL

FTO/glass substrates were cleaned by sonication in acetone, toluene, acetone, ethanol, and deionized water sequentially, and were subjected to UV ozone treatment for 5 min before use. ZnO ETL was prepared by both solution process and electron beam deposition. ZnO ETL was prepared via both solution process and electron beam deposition. For the solution approach, a sol-gel precursor solution was prepared by dissolving zinc acetate in 2-methoxyethanol at 40 mg/mL with the addition of 3 wt% ethanolamine. The precursor solution was stirred at 80 °C for 1 hour before use. The ZnO compact layer was synthesized by spin coating the precursor solution at 3000 rpm for 30s, followed by preheating at 150 °C for 5 min and annealing at 350 °C for 1 hour. For electron beam deposition approach, a 15 nm of ZnO layer was deposited on FTO/glass substrates at 180 °C.

2.3 Surface treatment of different ZnO ETL

Solution processed ZnO compact layers were subjected to different surface treatments. For PEI and PVP treatment, ZnO samples were immersed in the surfactant solution (0.1 wt% of PEI and PVP dissolved in isopropanol respectively) for 8 hours. For EA treatment, EA was dissolved in 2-methoxyethanol at 1 wt% and spin coated on ZnO surface at 3000 rpm for 30 s, followed by annealing at 130 °C for 10 min. For UV ozone treatment, as synthesized ZnO samples were subjected to UV ozone for 20 min.

2.4 Fabrication of ZnO based devices

$CH_3NH_3PbI_3$ perovskite films were synthesized by a conventional 2-step method.[8] PbI_2 was dissolved in DMF at a concentration of 1 M and stirred at 70 degree for 2 hours, while MAI was dissolved in isopropanol at 30 mg/mL at room temperature. PbI_2 solution was first spin coated on ZnO compact layers with or without surface treatment at 3000 rpm for 30 s, followed by drying at 70 °C on a hot plate for 20 min. MAI solution was then applied onto PbI_2 layer and waited for 1 min before spin coating at 3000 rpm for 30 s. Finally the substrates were annealed at 70 °C for 30 min. For hole transporting layer (HTL), a precursor solutions as prepared by dissolving 72.3 mg of spiro-OMeTAD in 1 mL of chlorobenzene solution with 28.8 μL 4 tert-butylpyridine and 17.5μL Li-TFSI solution (520 mg Li-TFSI in 1 mL acetonitrile). The precursor solution was spin coated on perovskite film at 4000 rpm for 30 s and then annealed at 40 °C in oxygen atmosphere for 1 hour. Finally, 15 nm of MoO_3 and 50 nm of Al were successively deposited as the contact electrodes via thermal evaporation.

2.5 Materials and Device characterization

Morphological characterization of perovskite films synthesized on different ETL was performed using a JEOL JMS-7001F scanning electron microscope. XPS measurement of ZnO layers was performed using a Thermo Fisher ESCALAB 250X XPS system. Photovoltaic performance of different devices was evaluated by measuring the current-

voltage (I-V) curves under simulated AM 1.5G illumination from ABET Sun 2000 solar simulator at a power density of 100 mW/cm^2. All devices were encapsulated in an inert atmosphere inside the glovebox before characterization. The J-V curves were obtained by scanning in the range between 1.2 V and -0.2 V at a scan rate of 1 V/s.

2.6 Accelerated stability testing

The stability of devices with solution processed ZnO ETL and electron beam deposited ZnO ETL were tested at 85 °C and 65% relative humidity in ambient environment. Encapsulated devices at open circuit were exposed under continuous AM 1.5G illumination at 100 mW/cm^2 for 48 hours. Power conversion efficiency of the devices were measured at specified time intervals.

3. RESULTS AND DISCUSSION

Figure 1 shows the SEM image of perovskite films synthesized on solution processed and electron beam deposited ZnO compact layers respectively. It can be observed that the morphologies of the obtained perovskite films exhibit significant differences. Perovskite films on solution processed ZnO compact layer have larger and evenly sized grains, while a rough film with small and unevenly distributed grains are observed for samples synthesized on electron beam deposited ZnO layers. The J-V curves of the best performing devices based on these two ZnO ETLs are shown in Figure 2. The cells based on solution processed ZnO ETL exhibit short circuit current density J_{sc} of 17.8±3.2 mA/cm^2, open circuit voltage V_{oc} of 1.06±0.03 V, and fill factor FF of 0.58±0.07, resulting in power conversion efficiency (PCE) of 11.0±2.8% under the condition of reverse scan. On the other hand, devices based on electron beam deposited ZnO ETL exhibit inferior photovoltaic performance, with with J_{sc}=19.6±6.3 mA/cm^2, V_{oc}=0.95±0.02 V, FF=0.58±0.07, and resulting PCE=8.4±1.8% under reverse scan.
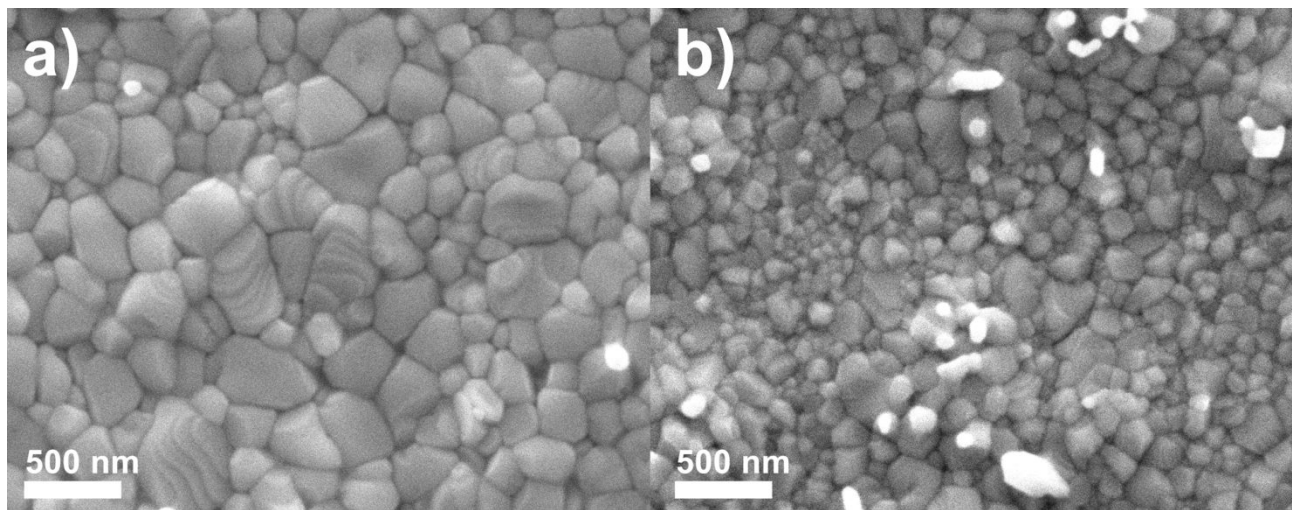

Figure 1. SEM images of perovskite films synthesized on a) solution processed ZnO ETL and b) electron beam deposited ZnO ETL.
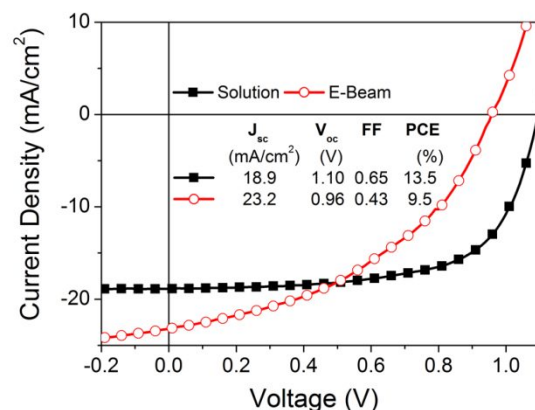
Figure 2. I-V characterization of devices with ZnO ETL prepared by different approaches.

Furthermore, devices with different ZnO ETL were subjected to continuous illumination at 85 °C for 48 hours to evaluate the influence of ZnO ETL on device stability. Figure 3 shows the PCE of the devices as a function of time. Regarding the device with electron beam deposited ZnO ETL, significant efficiency drop is observed within the first 3 hours of the stability testing, with a PCE approaching 10% of the initial PCE after 48 hours. On the other hand, device with solution processed ZnO ETL exhibit slightly higher stability, with the PCE gradually decreases to 30% of the initial PCE after 48 hours. Both devices with solution processed ZnO ETL and electron beam deposited ZnO ETL exhibit inferior stability compared to conventional TiO_2 based devices, which is in agreement with the previous report.[8]
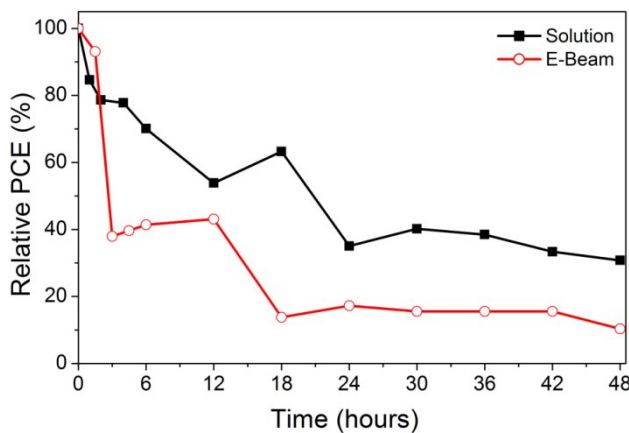

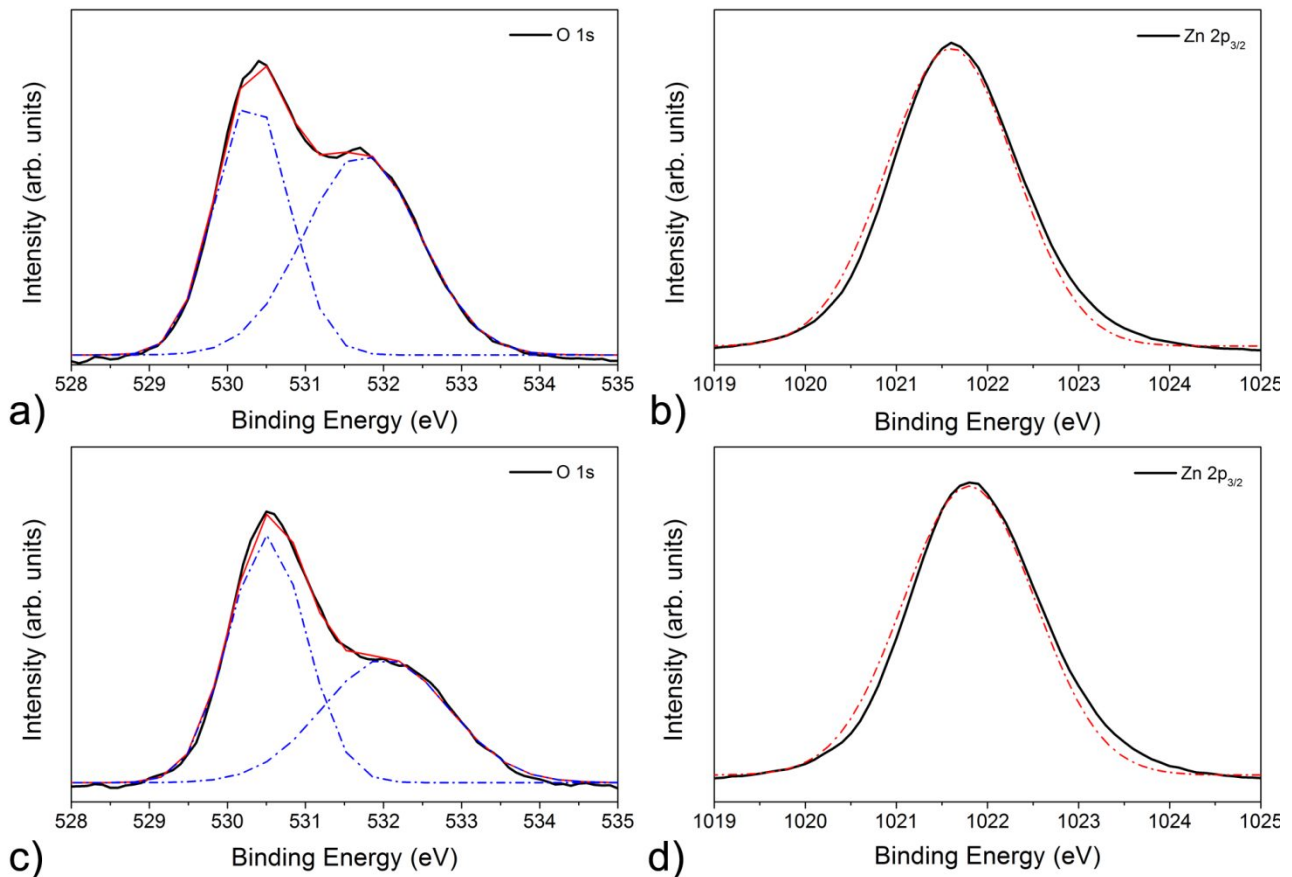Figure 3. PCE of devices with ZnO ETL prepared by different approaches as a function of time.

Figure 4. XPS spectra of a) O 1s and b) ZnO 2p$_{3/2}$ of solution processed ZnO film, c) O 1s and d) Zn 2p$_{3/2}$ of electron beam deposited ZnO film respectively.

XPS measurements were performed to investigate the surface composition of the ZnO samples prepared by two different approaches, with the results summarized in Figure 4. The XPS spectra were calibrated with the carbon 1s peak located at 285 eV as a reference position. For both ZnO samples, the O 1s spectra can be resolved as a superposition of two Gaussian components corresponding to different oxygen environments in the ZnO sample. The peak located at lower binding energy (~530.4 eV, denoted as O1) is corresponding to oxygen in ZnO lattice, while the peak centered at ~531.7 eV (denoted as O2) is usually attributed to O^{2-} ions in oxygen-deficient regions or loosely bound oxygen on the surface such as OH groups.[14] Slight difference in O2 peak positions (531.7 eV for solution processed ZnO and 532.0 eV for electron beam deposited ZnO) can be observed. In addition, variation in the relative composition of O1 and O2 peaks can be observed between the two ZnO samples. Therefore, the XPS results indicate differences in the surface composition of ZnO compact layers prepared by different methods, which may be further linked to the variation in the surface adsorbates and defects of ZnO samples. Regarding the devices with ZnO ETL prepared by different methods, it is likely that the defects and adsorbates at ZnO/perovskite interfaces affect the electron transport and consequently the photovoltaic performance of the resulted devices.
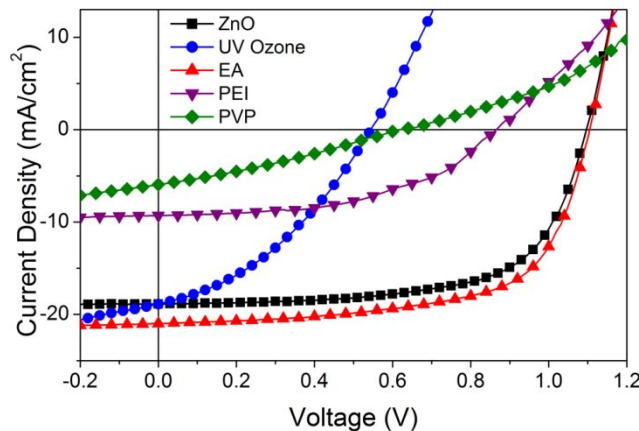
Figure 5. I-V characterization of devices with solution processed ZnO ETL subjected to different surface treatments.

Since the surface properties of ZnO compact layer may predominantly affect the electron injection and transport at ZnO/perovskite interfaces, direct surface modification of the ZnO ETL is expected to alter the surface properties and hence vary the resulting device performance. In this work, several surface modification approaches are applied to the solution processed ZnO layer, including UV ozone treatment with extended treatment time as well as various surface modification agents. The J-V curves for the devices with different surface treatment are shown in Figure 5. It can be observed from the results that extended UV ozone treatment does not result in a positive effect on device performance, although UV ozone is expected to reduce the organic contamination on the surface of ZnO layer. Device with UV ozone treatment, though with similar J_{sc} compared to the control sample, exhibits significantly decreased V_{oc} resulting in poor energy conversion efficiency. Neither PEI nor PVP treatments result in enhancement in photovoltaic performance, with significantly reduced J_{sc} and V_{oc} in the the resulting devices. This is likely attributed to the increase in the series resistance by introducing a polymer agent at the ZnO/perovskite interface. On the other hand, EA treatment resulted in an improvement in the device efficiency with increased J_{sc} and fill factor compared to the device with unmodified ZnO ETL.

Figure 6 shows the SEM images of the perovskite films synthesized on ZnO compact layer with EA treatment. Negligible difference is observed compared to the morphology of perovskites synthesized on unmodified ZnO. Figure 7 shows the J-V curves under both reverse scan and forward scan for ZnO based devices with or without EA treatment. Under reverse scan, increase in J_{sc}, V_{oc}, as well as fill factor can be observed in the device with EA treatment, leading to a significant enhancement in the overall energy conversion efficiency exceeding 15% for the best performing device. In addition, hysteresis effect is reduced under forward scan for the EA-treated device. Therefore, EA treatment is likely an effective surface modification approach leading to the improvement in device performance which could be explained as the passivation of ZnO surface defects by EA treatment resulting in reduced recombination at ZnO/perovskite interface. Nevertheless, even with the impressive enhancement due to EA treatment, the obtained ZnO based devices are still outperformed by most TiO_2 based devices. Further investigation on manipulating ZnO surface to passivate surface defects and thus reduce recombination loss at ZnO/perovskite interfaces is essential to improve the photovoltaic performance of ZnO based PSCs.
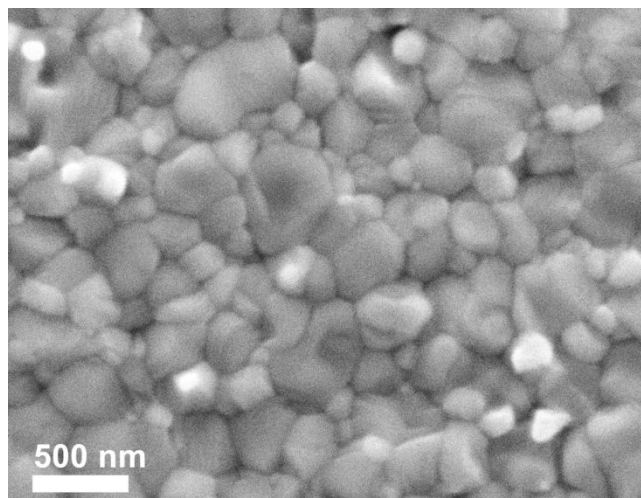
Figure 6. SEM image of perovskite film synthesized on ZnO ETL with EA surface treatment.
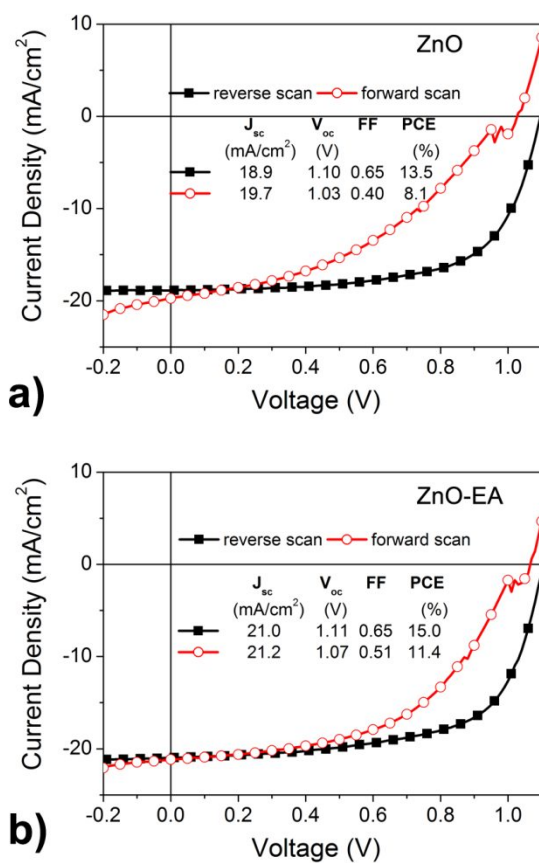

Figure 7. I-V characterization of the best performing devices corresponding to a) solution processed ZnO ETL, and b) solution processed ZnO ETL with EA surface treatment.

4. CONCLUSIONS

In this work, the effect of ZnO deposition methods and post-deposition treatments on the perovskite film properties, device performance and stability is investigated. It can be indicated that the deposition methods and direct surface modifications have prominent influence on ZnO surface properties, which are further linked to the properties of ZnO/perovskite interface, perovskite film quality, and consequently the efficiencies of the resulting devices. EA treatment is demonstrated to have a favorable effect on passivating ZnO surface defects and thus improving photovoltaic performance of ZnO based devices. Further study on surface modification of ZnO ETL is necessary to achieve better energy conversion efficiencies.

Acknowledgement

REFERENCES

[1] Jung, H. S., Park, N.-G., "Perovskite solar cells: From materials to devices," *Small* 11, 10-25 (2015).

[2] Kim, H.-S. Lee, C.-R., Im, J.-H., Lee, K.-B., Moehl, T., Marchioro, A., Moon, S.-J., Humphry-Baker, R., Yum, J.-H., Moser, J. E., Grätzel, M., and Park, N.-G., "Lead iodide perovskite sensitized all-solid-state submicron thin film mesoscopic solar cell with efficiency exceeding 9%," *Sci. Rep.* 2, 591 (2012).

[3] Lee, M. M., Teuscher, J., Miyasaka, T., Murakami, T. N., and Snaith, H. J., "Efficient hybrid solar cells based on meso-superstructured organometal halide perovskites," *Science* 338, 643-674 (2012).

[4] "Best Research-Cell Efficiencies," NREL, http://www.nrel.gov/ncpv/images/efficiency_chart.jpg (5 January 2017).

[5] Son, D.-Y., Im, J.-H., Kim, H.-S., and Park, N.-G., "11% efficient perovskite solar cell based on ZnO nanorods: An effective charge collection system," *J. Phys. Chem. C* 118, 16567-16573 (2014).

[6] Mahmood, K., Swain, B. S., and Amassian, A., "16.1% efficient hysteresis-free mesostructured perovskite solar cell based on synergistically improved ZnO nanorod arrays," *Adv. Energy Mater.* 5, 1500568 (2015).

[7] Kumar, M. H., Yantara, N., Dharani, S., Grätzel, M., Mhaisalkar, S., Boix, P. P., and Mathews, N., "Flexible, low-temperature, solution processed ZnO-based perovskite solid state solar cells," *Chem. Commun.* 49, 11089-11091 (2013).

[8] Dong, Q., Liu, F. Z., Wong, M. K., Tam, H. W., Djurišić, A. B., Ng, A., Surya, C., Chan, W. K., and Ng, A. M. C., "Encapsulation of perovskite solar cells for high humidity conditions, " *ChemSusChem* 9, 2597-2603 (2016).

[9] Dkhissi, Y., Meyer, S., Chen, D., Weerasinghe, H. C., Spiccia, L., Cheng, Y.-B., and Caruso, R. A., "Stability comparison of perovskite solar cells based on zinc oxide and titania on polymer substrates," ChemSusChem 9, 687-695 (2016).

[10] Yang, J., Siempelkamp, B. D., Mosconi, E., De Angelis, F., and Kelly, T. L., "Origin of the thermal instability in $CH_3NH_3PbI_3$ thin films deposited on ZnO," *Chem. Mater.* 27 4229-4236 (2015).

[11] Guo, Y., Li, X., Kang, L. L., He, X., Ren, Z. Q., Wu, J. D., and Qi, J. Y., "Improvement of stability of ZnO/ $CH_3NH_3PbI_3$ bilayer by aging step for preparing high-performance perovskite solar cells under ambient conditions," RSC Adv. 6, 62522-62528 (2016).

[12] Si, H. N., Liao, Q. L., Zhang, Z., Li, Y., Yang, X. H., Zhang, G. J., Kang, Z., Zhang, Y., "An innovative design of perovskite solar cells with Al_2O_3 inserting at ZnO/perovskite interface for improving the performance and stability," *Nano Energy* 22, 223–231 (2016).

[13] Dong, J., Zhao, Y. H., Shi, J. Q., Wei, H. Y., Xiao, J. Y., Xu, X., Luo, J. H., Xu, J., Li, D. M., Luo, Y. H., and Meng, Q. B., "Impressive enhancement in the cell performance of ZnO nanorod-based perovskite solar cells with Al-doped ZnO interfacial modification," *Chem. Commun.* 50, 13381-13384 (2014).

[14] Chen, C., He, H. P., Lu, Y. F., Wu, K. W., and Ye, Z. Z., "Surface passivation effect on the photoluminescence of ZnO nanorods," ACS Appl. Mater. Interfaces 5, 6354-6359 (2013).

[15] Yu, J. C., Kim, D. B., Baek, G., Lee, B. R., Jung, E. D., Lee, S., Chu, J. H., Lee, D.-K., Choi, K. J., Cho, S., and Song, M. H., "High-performance planar perovskite optoelectronic devices: A morphological and interfacial control by polar solvent treatment," *Adv. Mater.* 27, 3492-3500 (2015).